

ON THE ACCURACY OF MFIE AND CFIE IN THE SOLUTION OF LARGE ELECTROMAGNETIC SCATTERING PROBLEMS

Özgür Ergül¹ and Levent Gürel^{1,2}

¹Department of Electrical and Electronics Engineering, Bilkent University, TR-06800, Ankara, Turkey

²Computational Electromagnetics Research Center (BiLCEM), Bilkent University, TR-06800, Ankara, Turkey

Email: ergul@ee.bilkent.edu.tr; lgurel@bilkent.edu.tr

ABSTRACT

We present the linear-linear (LL) basis functions to improve the accuracy of the magnetic-field integral equation (MFIE) and the combined-field integral equation (CFIE) for three-dimensional electromagnetic scattering problems involving large scatterers. MFIE and CFIE with the conventional Rao-Wilton-Glisson (RWG) basis functions are significantly inaccurate even for large and smooth geometries, such as a sphere, compared to the solutions by the electric-field integral equation (EFIE). By using the LL functions, the accuracy of MFIE and CFIE can be improved to the levels of EFIE without increasing the computational requirements and with only minor modifications in the existing codes based on the RWG functions.

Key words: Magnetic-field integral equation; combined-field integral equation; scattering problems; basis functions; multilevel fast multipole algorithm.

1. INTRODUCTION

The accuracy problem of the magnetic-field integral equation (MFIE) and the combined-field integral equation (CFIE) [1] with Rao-Wilton-Glisson (RWG) [2] basis functions applied on large scattering problems is reported. Our recent studies on the inaccuracy of MFIE for moderate-size problems have shown that the source of the error is the RWG functions and the accuracy can be improved by decomposing the RWG functions into first-order-complete linear-linear (LL) basis functions [3],[4]. On the other hand, it was thought that the accuracy problem was limited to small geometries, especially those including sharp edges and corners. In this work, we show that MFIE and CFIE with the RWG functions are significantly inaccurate even for large and smooth geometries, such as a sphere, and the accuracy can again be improved with the LL functions. For the solution of large problems, implementations of multilevel fast multipole algorithm (MLFMA) [5] employing LL functions are also presented.

2. INACCURACY OF MFIE AND CFIE FOR SMOOTH GEOMETRIES

In the solution of three-dimensional electromagnetic scattering problems by the method of moments (MOM), it is common to apply a triangulation on the scatterer and employ RWG basis functions defined on planar triangles to expand the unknown surface current density. The scattering problem can be formulated by three different integral equations, i.e., the electric-field integral equation (EFIE), MFIE, and CFIE. Although the same physical current distribution is expanded by an identical set of RWG functions in all cases, the same levels of accuracy cannot be obtained by the three integral equations. Independent of the shape of the geometry (smooth or sharp), MFIE and CFIE with the RWG functions have consistent errors that produce worse results than EFIE [6].

As an example to the inaccuracy of MFIE and CFIE with the RWG functions, Fig. 1 presents the forward-scattered radar cross section (RCS) values for the sphere geometry. The radius of the sphere varies from λ to 2λ and the RCS is plotted with respect to a ratio of the radius to wavelength. All the computational curves are obtained by a sphere model obtained by $\lambda/10$ triangulation with respect to the largest frequency and RWG functions are employed to expand the unknown current density. Fig. 1(a) presents the EFIE solution, which is quite accurate compared to the analytical solution obtained by Mie series. However, this is not true for the MFIE solution depicted in Fig. 1(b), where the computational curve deviates from the analytical values. In the case of MFIE, there are two significant error sources in the computation of the scattered fields, namely, the internal resonances and the insufficiency of the RWG functions to discretize the MFIE kernel. The internal resonances are clearly observed in Fig. 1(b) as dips on the curves. On the other hand, MFIE inaccuracy due to the RWG functions also appears as a general deviation from the analytical curve for all frequencies. Finally, the internal resonance disappears for CFIE but the error due to the RWG functions remains as presented in Fig. 1(c) through the contribution of MFIE in CFIE.

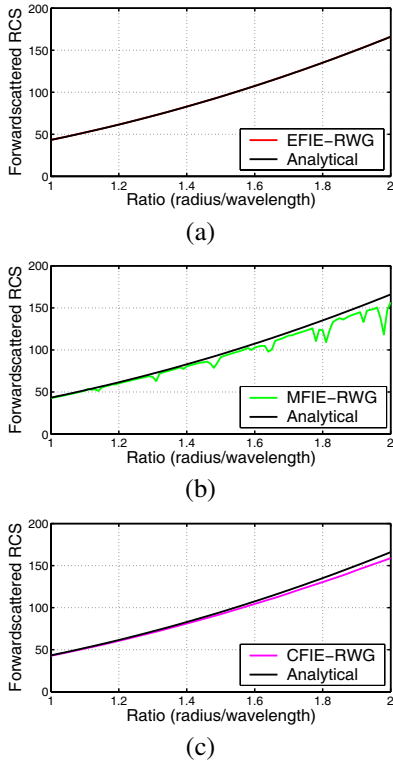


Figure 1. Forward-scattered RCS values of the sphere geometry as a function of ratio of radius to wavelength obtained by (a) EFIE, (b) MFIE, and (c) CFIE employing RWG functions. Analytical values obtained by a Mie series solution are also plotted for comparisons.

Next, we present the relative error in the forward-scattered RCS in Fig. 2 as a function of radius per wavelength. Although the relative error of the EFIE solution is below 10^{-3} , MFIE and CFIE results obtained by the same discretization of the geometry have considerably larger errors. As discussed above, the error due to the RWG functions exists both for MFIE and CFIE, but MFIE also suffers from the internal resonance problems. These resonances of MFIE appear in Fig. 2 as peaks above a base formed by the CFIE curve. Finally, Fig. 3 presents the relative error in the bistatic RCS as a function of bistatic angle and ratio of radius to wavelength. In these two-dimensional plots, 0° and 180° correspond to backscattering and forward-scattering directions, respectively. In addition, red and blue colors represent the high and low relative errors, respectively. In Fig. 3(a), relative error of EFIE is rarely above 10^{-2} , which occurs due to zero-crossings of the bistatic RCS. In the case of the MFIE in Fig. 3(b), internal resonances are clearly visible as vertical red lines in the two-dimensional plot. However, the error is higher than the error of EFIE also in other frequencies. Finally, Fig. 3(c) clearly shows the error of CFIE when compared to the EFIE result in Fig. 3(a).

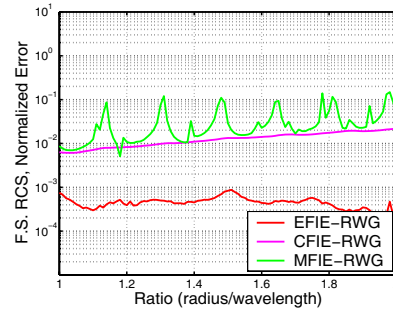


Figure 2. Relative errors in the forward-scattered RCS values of the sphere geometry as a function of ratio of radius to wavelength calculated by EFIE, MFIE, and CFIE employing RWG functions. Errors are calculated with respect to analytical values.

3. IMPROVING THE ACCURACY OF MFIE AND CFIE USING LINEAR-LINEAR BASIS FUNCTIONS

Linear-linear (LL) basis functions are employed in [4] to improve the accuracy of the MFIE and CFIE implementations. Contrary to the RWG functions, LL functions are first-order complete to represent the vectors by providing six degrees of freedom to model the linear variation on the triangles [7]. As depicted in Fig. 4, there are two kinds of LL functions defined on the same edge simultaneously to expand the current density better than the RWG functions that are only zeroth-order complete. Improved current modelling with higher-order completeness is achieved at the cost of doubling the number of basis functions compared to the RWG functions for the same triangulation of the geometry. On the other hand, LL functions provide more accurate results with MFIE and CFIE for the same number of unknowns as the RWG functions. In this section, we show that the improvement is also obtained to correct the inaccuracy of MFIE and CFIE in the formulations and solutions of smooth geometries.

Fig. 5 presents the MFIE and CFIE solutions of the sphere obtained by employing LL functions. Compared to Figs. 1(b) and (c), we observe that the forward-scattered RCS values are significantly improved and they become as accurate as the EFIE solution in Fig. 1(a). In addition, Fig. 6 depicts the MFIE and CFIE errors with the LL functions and they are compared to the EFIE error with the RWG functions. We observe that all three solutions have the same accuracy except for the unavoidable internal resonances of MFIE. Finally, Fig. 7 presents the relative error in the bistatic RCS for the MFIE and CFIE implementation employing the LL functions. Comparing Fig. 7(a) to Fig. 3(b), we observe two consequences when the RWG functions are replaced by the LL functions for the MFIE implementations. First, the effects of internal resonances are narrower as a function of frequency for the LL functions. Second, the error of MFIE due to the RWG functions disappears and the accuracy is improved for all frequencies. The

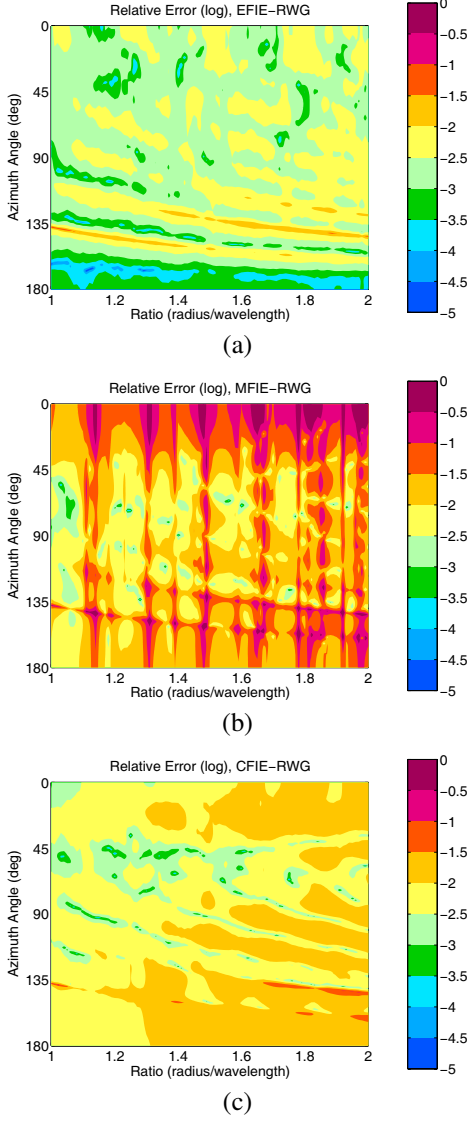


Figure 3. Relative error in the bistatic RCS of the sphere geometry calculated by (a) EFIE, (b) MFIE, and (c) CFIE employing RWG functions.

improvement obtained by the LL functions for CFIE is also clearly visible when Fig. 7(b) is compared to Fig. 3(c). By employing the LL functions, the CFIE error is now in the levels of EFIE error displayed in Fig. 3(a).

4. EMPLOYING LINEAR-LINEAR BASIS FUNCTIONS FOR THE SOLUTIONS OF LARGE SCATTERING PROBLEMS

For the solution of large problems, we implemented MLFMA employing LL functions as the basis and testing functions. The fundamental idea in MLFMA is to replace element-to-element interactions with cluster-to-cluster interactions in a multilevel scheme. This computational scheme relies on the factorization of the Green's

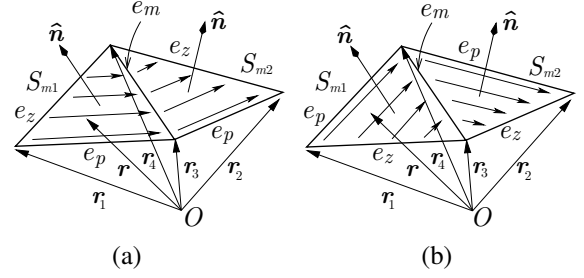


Figure 4. (a) First-kind and (b) second-kind LL functions defined on the edge e_m .

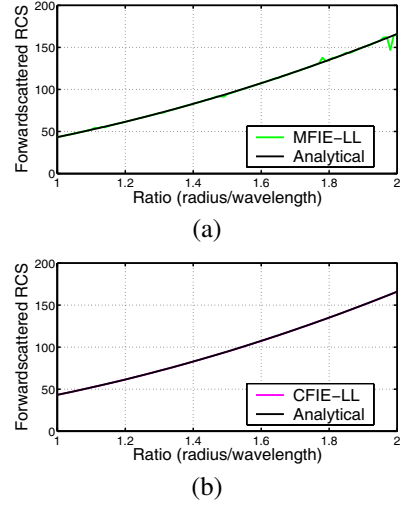


Figure 5. Forward-scattered RCS values of the sphere geometry as a function of ratio of radius to wavelength obtained by (a) MFIE and (b) CFIE employing LL functions. Analytical values obtained by a Mie series solution are also plotted for comparisons.

function, which is valid only for basis and testing functions that are far from each other. For the far-field interactions, the matrix elements are derived as [5]

$$Z_{mn}^E = \frac{ik}{(4\pi)^2} \int d^2\hat{\mathbf{k}} \mathbf{F}_{C_m}^{E,rec}(\hat{\mathbf{k}}) T_L(\mathbf{k}, \mathbf{D}) \cdot \mathbf{F}_{C'_n}^{E,rad}(\hat{\mathbf{k}}) \quad (1)$$

for EFIE and

$$Z_{mn}^M = \frac{k}{(4\pi)^2} \int d^2\hat{\mathbf{k}} \mathbf{F}_{C_m}^{M,rec}(\hat{\mathbf{k}}) T_L(\mathbf{k}, \mathbf{D}) \cdot \mathbf{F}_{C'_n}^{M,rad}(\hat{\mathbf{k}}) \quad (2)$$

for MFIE, where $\hat{\mathbf{k}}$ is the angular direction on the unit sphere, k is the wavenumber, and

$$T_L(\mathbf{k}, \mathbf{D}) = \sum_{l=0}^L i^l (2l+1) h_l^{(1)}(kD) P_l(\hat{\mathbf{D}} \cdot \hat{\mathbf{k}}) \quad (3)$$

is the translation function written in terms of the spherical Hankel function of the first kind $h_l^{(1)}$ and Legendre polynomial P_l .

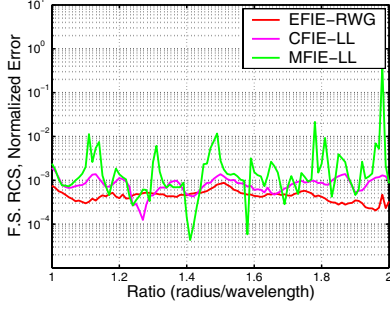


Figure 6. Relative errors in the forward-scattered RCS values of the sphere geometry as a function of ratio of radius to wavelength calculated by MFIE and CFIE employing LL functions. Errors are calculated with respect to analytical values.

In (1) and (2), $\mathbf{F}_{Cm}^{E,rec}$ and $\mathbf{F}_{Cm}^{M,rec}$ represent the receiving patterns of the m th testing function with respect to a close point C for EFIE and MFIE, respectively. Similarly, $\mathbf{F}_{C'n}^{E,rad}$ and $\mathbf{F}_{C'n}^{M,rad}$ are the radiation patterns of the n th basis function with respect to a close point C' . The translation function in (3) evaluates the interaction between the basis and testing groups that are located at C' and C , respectively, and separated by

$$\mathbf{D} = |\mathbf{D}|\hat{\mathbf{D}} = \mathbf{r}_C - \mathbf{r}_{C'}. \quad (4)$$

As an example, we consider the LL functions of the first kind depicted in Fig. 4(a) and take only the first triangles of the basis and testing functions to derive the radiation and receiving patterns. Then, EFIE and MFIE radiation patterns are derived as

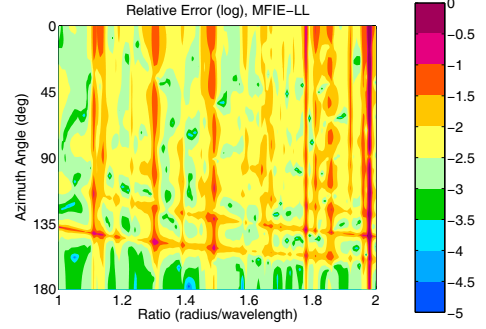
$$\begin{aligned} \mathbf{F}_{C'n1}^{E,rad}(\hat{\mathbf{k}}) &= \mathbf{F}_{C'n1}^{M,rad}(\hat{\mathbf{k}}) \\ &= \int_{S_{n1}} d\mathbf{r}' e^{-i\mathbf{k}\cdot(\mathbf{r}'-\mathbf{r}_{C'})} (\mathbf{I} - \hat{\mathbf{k}}\hat{\mathbf{k}}) \cdot \mathbf{b}_n(\mathbf{r}') \\ &= (\mathbf{I} - \hat{\mathbf{k}}\hat{\mathbf{k}}) \cdot \mathbf{B}_{n1} \cdot \int_{S_{n1}} d\mathbf{r} e^{-i\mathbf{k}\cdot(\mathbf{r}'-\mathbf{r}_{C'})} (\mathbf{r}' - \mathbf{r}_1), \end{aligned} \quad (5)$$

where

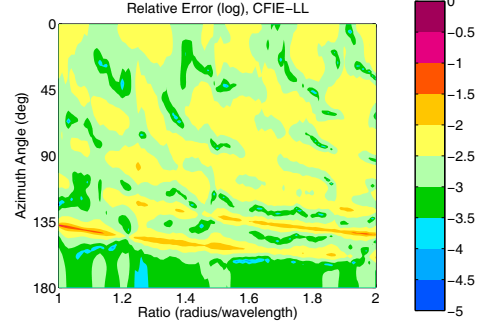
$$\mathbf{B}_{n1} = \frac{l_n}{4(A_{n1})^2} (\mathbf{r}_3 - \mathbf{r}_1) [(\mathbf{r}_4 - \mathbf{r}_1) \times \hat{\mathbf{n}}]. \quad (6)$$

Similarly, EFIE and MFIE receiving patterns are derived as

$$\begin{aligned} \mathbf{F}_{Cm1}^{E,rec}(\hat{\mathbf{k}}) &= [\mathbf{F}_{Cm1}^{E,rad}(\hat{\mathbf{k}})]^* \\ &= \int_{S_{m1}} d\mathbf{r} e^{i\mathbf{k}\cdot(\mathbf{r}-\mathbf{r}_C)} (\mathbf{I} - \hat{\mathbf{k}}\hat{\mathbf{k}}) \cdot \mathbf{t}_m(\mathbf{r}) \\ &= (\mathbf{I} - \hat{\mathbf{k}}\hat{\mathbf{k}}) \cdot \mathbf{B}_{m1} \cdot \int_{S_{m1}} d\mathbf{r} e^{i\mathbf{k}\cdot(\mathbf{r}-\mathbf{r}_C)} (\mathbf{r} - \mathbf{r}_1) \end{aligned} \quad (7)$$



(a)



(b)

Figure 7. Relative error in the bistatic RCS of the sphere geometry calculated by (a) MFIE and (b) CFIE employing LL functions.

and

$$\begin{aligned} \mathbf{F}_{Cm}^{M,rec}(\hat{\mathbf{k}}) &= -\mathbf{k} \times \int_{S_m} d\mathbf{r} e^{i\mathbf{k}\cdot(\mathbf{r}-\mathbf{r}_C)} \mathbf{t}_m(\mathbf{r}) \times \hat{\mathbf{n}} \\ &= -\mathbf{k} \times \mathbf{B}_{m1} \times \hat{\mathbf{n}} \cdot \int_{S_{m1}} d\mathbf{r} e^{i\mathbf{k}\cdot(\mathbf{r}-\mathbf{r}_C)} (\mathbf{r} - \mathbf{r}_1), \end{aligned} \quad (8)$$

respectively. In (5)-(8), the integrals are evaluated analytically and they are the same as those involved in the RWG implementations. The derivations related to the second triangles and for the LL functions of the second kind are similar.

5. IMPROVING THE ACCURACY OF MFIE AND CFIE FOR THE SOLUTION OF LARGE PROBLEMS

Fig. 8 presents the solution of the scattering problems involving a sphere of radius 6λ . The problems formulated by CFIE are solved by MLFMA implementations employing RWG and LL functions. The sphere is discretized with mesh sizes of about $\lambda/8$ for RWG and $\lambda/5$ for LL. Then, the numbers of unknowns are approximately the same for the RWG and LL cases although the triangulation is coarser for the LL case. In Fig. 8, the bistatic RCS on the E-plane is plotted, where the analytical results are also displayed. Then, we calculate the absolute errors of computational results

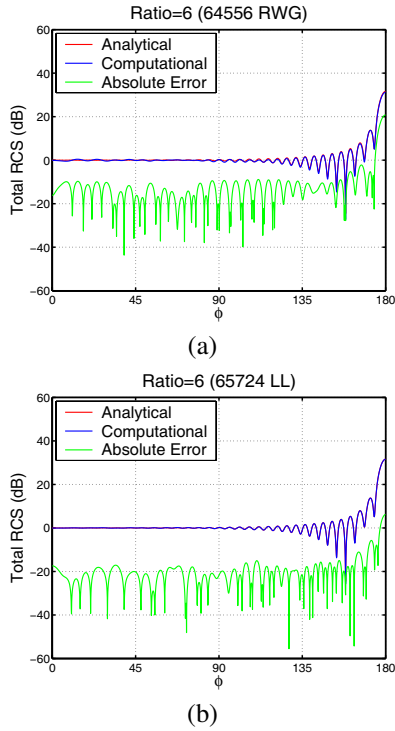


Figure 8. Bistatic RCS of a sphere of radius 6λ calculated by MLFMA employing CFIE and (a) RWG functions and (b) LL functions.

with respect to analytical values. Comparing Fig. 8(a) to Fig. 8(b), we observe the significant improvement by employing the LL functions.

To show that the RWG functions are actually insufficient for MFIE and CFIE, Table 1 lists the relative errors compared to the Mie-series solution. In the computational solutions, the numerical integrals on the basis and testing functions are evaluated with at most 1% error and the far-field interactions are calculated with three digits of accuracy. However, when the RWG functions are employed, $\lambda/10$ triangulation leads to 3.59% and 2.17% errors in the MFIE and CFIE solutions, respectively. This inaccuracy is unacceptable considering all the efforts for controlling errors in the MLFMA implementations. We note that the relative error decreases below 1% by employing 528,786 RWG functions. On the other hand, only 65,724 LL functions corresponding to triangulation with $\lambda/5$ mesh size give more accurate results in spite of coarser modelling of the curvatures. Comparing the number of unknowns required for the same level of accuracy, it is observed that the LL functions are more efficient compared to the RWG functions for MFIE and CFIE.

6. CONCLUSION

We report the accuracy problem of MFIE and CFIE with the RWG basis functions for the solutions of large scattering problems by MLFMA. MFIE and CFIE with the

Table 1. Relative Errors in the Forward-Scattering RCS Values for a Sphere of Radius 6λ

Triangulation	Unknowns	MFIE	CFIE
$\lambda/5$	64,556 RWG	7.39%	4.30%
$\lambda/10$	132,003 RWG	3.59%	2.17%
$\lambda/14$	270,225 RWG	1.60%	1.07%
$\lambda/20$	528,786 RWG	0.77%	0.57%
$\lambda/5$	65,724 LL	0.39%	0.23%

RWG functions are significantly inaccurate even for large and smooth geometries and the accuracy can be improved by replacing the RWG functions with the LL functions.

ACKNOWLEDGMENTS

This work was supported by the Scientific and Technical Research Council of Turkey (TUBITAK) under Research Grant 105E172, by the Turkish Academy of Sciences in the framework of the Young Scientist Award Program (LG/TUBA-GEBIP/2002-1-12), and by contracts from ASELSAN and SSM.

REFERENCES

- [1] A. J. Poggio and E. K. Miller, "Integral equation solutions of three-dimensional scattering problems," in *Computer Techniques for Electromagnetics*, R. Mittra, Ed. Oxford: Pergamon Press, 1973, Chap. 4.
- [2] S. M. Rao, D. R. Wilton, and A. W. Glisson, "Electromagnetic scattering by surfaces of arbitrary shape," *IEEE Trans. Antennas Propagat.*, vol. AP-30, no. 3, pp. 409–418, May 1982.
- [3] Ö. Ergül and L. Gürel, "Improving the accuracy of the MFIE with the choice of basis functions," in *Proc. IEEE Antennas and Propagation Soc. Int. Symp.*, vol. 3, 2004, pp. 3389–3392.
- [4] Ö. Ergül and L. Gürel, "Improving the accuracy of the magnetic-field integral equation with the linear-linear basis functions," *Radio Sci.*, vol. 41, RS4004, July 2006.
- [5] C.-C. Lu and W. C. Chew, "Multilevel fast multipole algorithm for electromagnetic scattering by large complex objects," *IEEE Trans. Antennas Propagat.*, vol. 45, no. 10, pp. 1488–1493, Oct. 1997.
- [6] Ö. Ergül and L. Gürel, "The use of curl-conforming basis functions for the magnetic-field integral equation," *IEEE Trans. Antennas Propagat.*, vol. 54, no. 7, pp. 1917–1926, July 2006.
- [7] L. C. Trintinalia and H. Ling, "First order triangular patch basis functions for electromagnetic scattering analysis," *J. of Electromagn. Waves and Appl.*, vol. 15, no. 11, pp. 1521–1537, 2001.